arXiv:1211.7001v1 [quant-ph] 29 Nov 2012

Pre-management of Non-local Decoherence

Xiao-Feng Qian*
Rochester Theory Center and Department of Physics & Astronomy
University of Rochester, Rochester, New York 14627

(Dated: November 30, 2012)

The possibility of pre-managing a non-local decoherence process with limited resources based on initial conditions is an open question. A generic two-qubit system that undergoes local but different amplitude-damping dissipations is studied to analyze the relation between entanglement sudden death (ESD) properties and initial conditions. ESD-free, ESD-tolerable and ESD-no-go phases are shown to be pre-manageable through the initial entanglement and excitation probabilities. Our results may provide useful guidance to state preparations in practice.

PACS numbers: 03.65.Ud, 03.65.Yz, 42.50.Pq, 75.10.Jm

BACKGROUND

Coherence is one of the central requirements for the success of quantum computation and quantum communication tasks [1]. However, the existence of unavoidable environmental interactions will induce both local and non-local decoherences [2]. In particular, this irreversible process may lead to the finite-time disappearance of non-local coherence [3] when local coherences still remain non-zero. This is well known as the entanglement sudden death (ESD) phenomenon [4]. In most cases, in order for a quantum information task to be successful, the ESD time scale ought to be much longer than the computation or operation time scale. Therefore an open challenge is to determine and control the timing of ESD.

A number of successful schemes, such as quantum error correction [5], feedback control [6], dynamical decoupling [7], etc, have been proposed during the last two decades in order to control and suppress the decay of local coherence. However, the decay of non-local coherence, i.e., entanglement, can be very different and inconsistent with local decoherence [8]. Consequently, several recent studies [9–11] based on different schemes have revealed that while these proposals may delay the occurrence of ESD in some cases, they may also counter-intuitively accelerate or even induce ESD. Decoherence free subspace [12] is another category of strategy. However, it would either cost an increased number of non-computing qubits to create certain symmetry, or some serious engineering of the system or reservoir with external contacts (equivalent to dynamical decoupling [13]) that might bring in additional source of noise to neighboring qubits. A more reliable, simpler, and systematic method to delay or even avoid ESD would be desirable.

Most of the prior treatments are managed during the decoherence and/or disentanglement process. An interesting question is whether ESD can be pre-managed before it is taking place, i.e., during the state preparation process. Recently we have given a trial answer to this question for a type of simple form two-qubit states. We showed that ESD properties are determined by a couple of initial parameters, i.e., entanglement and double excitation probability or purity [14]. It is also shown that ESD and initial pure states of a two-qubit system (under identical noisy channels) are statistically related [15]. For practical situations, the initial state may not be simple and pure, and the reservoirs may not be identical. Then a key question arises: is it still possible to manage ESD with only a few controllable initial parameters.

In this paper we extend the analysis to arbitrary two-qubit mixed states, and treat decoherence via local different amplitude-damping dissipations. We decompose the mixed state into its “X” and “O” components [16, 17], and first analyze the X-form component. This is a legal density matrix by itself and its entanglement properties were first studied by Yu and Eberly [18]. We show that the exact ESD-free, ESD-tolerable and ESD-no-go phases of the X-form matrix are explicitly determined, and thus manageable, through several of its initial parameters, i.e., entanglement and excitation probabilities.

We then apply the static entanglement boundary relation for X-form matrices, developed recently by Ma et al. [16] and by Hashemi Rafsanjani and Agarwal [17], to the dynamical evolution of the state. They show that the ESD phase critical conditions of the X-form component simply provide lower bounds for those of the entire state X+O. Therefore the control of different ESD properties of a complicated state can be realized sufficiently through just a few initial parameters of its X-form component. Our results may provide guidance to experimental preparations of robust entangled states.

INITIAL STATE AND TIME EVOLUTION

In practice, state preparations will inevitably leave the system in mixed states. Thus we consider the most general form of a two-qubit (A and B) initial state

$$\rho(0) = \begin{pmatrix} \rho_{11} & \rho_{12} & \rho_{13} & \rho_{14} \\ \rho_{21} & \rho_{22} & \rho_{23} & \rho_{24} \\ \rho_{31} & \rho_{32} & \rho_{33} & \rho_{34} \\ \rho_{41} & \rho_{42} & \rho_{43} & \rho_{44} \end{pmatrix}, \tag{1}$$

which is expressed in the standard basis: $|e\rangle_A|e\rangle_B$, $|e\rangle_A|g\rangle_B$, $|g\rangle_A|e\rangle_B$, $|g\rangle_A|g\rangle_B$. Here $|e\rangle$ and $|g\rangle$ are usually interpreted as excited and ground states of qubits A, B. It is obvious that such a matrix can always be decomposed into a sum of X-form and O-form matrices, i.e., $\rho(0) = \rho_X(0) + O(0)$. Here

$$\rho_X(0) = \begin{pmatrix} \rho_{11} & 0 & 0 & \rho_{14} \\ 0 & \rho_{22} & \rho_{23} & 0 \\ 0 & \rho_{32} & \rho_{33} & 0 \\ \rho_{41} & 0 & 0 & \rho_{44} \end{pmatrix}, \tag{2}$$

has the X shape matrix elements [18], and $O(0)$ contains the remaining matrix elements that form an O shape. According to Refs. [16, 17], the entanglement in terms of concurrence [19] for the entire state is no less than that of its X-form component, i.e., $C[\rho(0)] \geq C[\rho_X(0)]$.

After the state preparation, the two qubits will inevitably interact with the environment and begin the process of dissipation. Here we consider the case when qubits A, B are subject independently to two different amplitude-damping channels, which may describe many physical realizations, e.g., spontaneous emission, spin chain Heisenberg interactions [20], etc. The evolution of the initial state can be described by Kraus operator representations [1], i.e.,

$$\rho(t) = \sum_{i=1}^{4} K_i(t)\rho(0)K_i^\dagger(t), \tag{3}$$

where the four joint Kraus operators $K_i(t)$, $i = 1, 2, 3, 4$, satisfying the relation $\sum_{i=1}^4 K_i(t)K_i^\dagger(t) = 1$, correspond to four possible tensor products of individual Kraus operators of qubits A, B, i.e., $K_i(t) = K_\mu^A \otimes K_\nu^B$, $\mu, \nu = 0, 1$.

For the amplitude-damping mechanism one has

$$K_0^A = \begin{pmatrix} \sqrt{q_a} & 0 \\ 0 & 1 \end{pmatrix}, \quad K_1^A = \begin{pmatrix} 0 & 0 \\ \sqrt{p_a} & 0 \end{pmatrix}, \tag{4}$$

where p_a is the excitation-transfer probability that grows from 0 to 1 irreversibly, and $q_a = 1 - p_a$ denotes the probability that qubit A remains in its excited state. The Kraus operators for qubit B are characterized similarly as (4) with decay probability q_b.

ESD PHASES FOR X-MATRIX

We first consider the dynamics of the X-form component (2), which can be regarded as an initial state by itself, and analyze its ESD properties. Later we will extend the static relation $C[\rho(0)] \geq C[\rho_X(0)]$ to the dynamical evolution of the entire arbitrary state (1), and show its ESD properties are manageable through the controllable parameters of the X-form component.

The degree of entanglement, i.e., concurrence, between the two qubits for the X-form initial state (2) takes a very compact form [18],

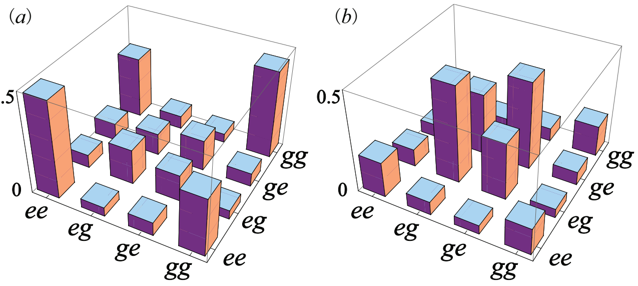

FIG. 1: Schematic illustration of two types of two-qubit matrices. For convenience the height of the cuboid represent the modulus of each matrix element. Plots (a) and (b) illustrate the Φ type ($Q_\Phi \geq Q_\Psi$) and Ψ type ($Q_\Psi > Q_\Phi$) of two-qubit matrices respectively.

$$C_0 = \max\{Q_\Phi, Q_\Psi, 0\}, \tag{5}$$

where

$$Q_\Phi = 2(|\rho_{14}| - \sqrt{\rho_{22}\rho_{33}}), Q_\Psi = 2(|\rho_{23}| - \sqrt{\rho_{11}\rho_{44}}). \tag{6}$$

Obviously, $C_0 = 0$ when $Q_\Phi < 0$ and $Q_\Psi < 0$. This is not an interesting case, so we will consider the cases when one of the Qs is positive (matrix positivity does not allow both Qs to be positive simultaneously). Then the initial concurrence is expressed conveniently as $C_0 = Q_\Phi$ for $Q_\Phi \geq Q_\Psi$, or $C_0 = Q_\Psi$ when $Q_\Psi > Q_\Phi$. Accordingly, we define the X-form matrix as well as the entire matrix (1) as a Φ matrix if $Q_\Phi \geq Q_\Psi$, or a Ψ matrix otherwise. An imperfect preparation of a Φ-like Bell state is a practical example of generating such a Φ matrix. Fig. 1 gives a schematic illustration of both types of matrices.

By applying the Kraus operators (4) to the initial state (2), one will obtain the time dependent state as

$$\rho_X(t) = \begin{pmatrix} \rho_{11}(t) & 0 & 0 & \rho_{14}(t) \\ 0 & \rho_{22}(t) & \rho_{23}(t) & 0 \\ 0 & \rho_{32}(t) & \rho_{33}(t) & 0 \\ \rho_{41}(t) & 0 & 0 & \rho_{44}(t) \end{pmatrix}, \tag{7}$$

where $\rho_{11}(t) = \rho_{11}q_aq_b$, $\rho_{22}(t) = \rho_{11}q_ap_b + \rho_{22}q_a$, $\rho_{33}(t) = \rho_{11}p_aq_b + \rho_{33}q_b$, $\rho_{44}(t) = \rho_{11}p_ap_b + \rho_{22}p_a + \rho_{33}p_b + \rho_{44}$, $\rho_{14}(t) = \rho_{41}^*(t) = \rho_{14}\sqrt{q_aq_b}$ and $\rho_{23}(t) = \rho_{32}^*(t) = \rho_{23}\sqrt{q_aq_b}$. The state retains an X form [18], and consequently the time dependent concurrence can be simply obtained as $C(t) = \max\{Q_\Phi(t), Q_\Psi(t), 0\}$, with

$$\begin{aligned} Q_\Phi(t) &= 2\sqrt{q_aq_b}(|\rho_{14}| - \sqrt{\Delta(t) + \rho_{22}\rho_{33}}), & (8) \\ Q_\Psi(t) &= 2\sqrt{q_aq_b}(|\rho_{23}| - \sqrt{\Delta(t) + \rho_{11}\rho_{44}}), & (9) \end{aligned}$$

and

$$\Delta(t) = \rho_{11}(\rho_{11}p_ap_b + \rho_{22}p_a + \rho_{33}p_b). \tag{10}$$

The irreversible damping process indicates that the product q_aq_b is decreasing and $\Delta(t)$ is increasing with time.

This guarantees the decay of both $Q_\Phi(t)$ and $Q_\Psi(t)$. Thus one has the time dependent concurrence, $C(t) = \max\{Q_\Phi(t), 0\}$ or $C(t) = \max\{Q_\Psi(t), 0\}$ for Φ or Ψ type of initial matrices respectively.

Φ type of X-matrix

Now we turn to the central task of this paper, and analyze the conditions of state (2) to avoid ESD, as well as the ESD onset conditions if it were to occur. We set $x_{ij} = \sqrt{\rho_{ii}\rho_{jj}}$ and $y_{ij} = \rho_{ii} + \rho_{jj}$ with $i, j = 1, 2, 3, 4$ for the convenience of our following notations.

For the Φ matrix situation, i.e., $C_0 = Q_\Phi \geq Q_\Psi$, the matrix positivity requires $Q_\Phi/2 \leq x_{14} - x_{23}$. This can be transformed in terms of the double excitation probability $D \equiv \rho_{11}$, and leads to the relation: $D_\Phi^{\min} \leq D \leq D_\Phi^{\max}$, where the physical boundaries are given as

$$\begin{aligned} 2D_\Phi^{\min} &= 1 - y_{23} - \sqrt{(1-y_{23})^2 - (Q_\Phi + 2x_{23})^2}, \\ 2D_\Phi^{\max} &= 1 - y_{23} + \sqrt{(1-y_{23})^2 - (Q_\Phi + 2x_{23})^2} \end{aligned} \quad (11)$$

Fig. 2 illustrates the behaviors of $D_\Phi^{\max}$ and $D_\Phi^{\min}$ with respect to Q_Φ by the upper red and lower blue solid lines respectively. The two boundary lines connect when $D = (1 - y_{23})/2$ and Q_Φ takes its maximum value $Q_\Phi^{\max} = 1 - y_{23} - 2x_{23}$ as illustrated by point 1 in plot (a).

From the quantity $Q_\Phi(t)$ given in (8), the condition to have ESD is whenever $\Delta(t) + x_{23}^2 \geq |\rho_{14}|^2$. There is no ESD at any time if $\Delta_{\max}(t) + x_{23}^2 \leq |\rho_{14}|^2$, where $\Delta_{\max}(t)$ is the maximum value of $\Delta(t)$ and is achieved when p_a, p_b take their maximum value 1 (usually corresponds to $t = \infty$). This ESD-free condition can be re-expressed in terms D bounded by its critical value D_Φ^f, i.e.,

$$D \leq D_\Phi^f = \left(\sqrt{y_{23}^2 + Q_\Phi^2 + 4x_{23}Q_\Phi} - y_{23}\right)/2. \quad (12)$$

Interestingly, D is only controlled by the system initial parameters Q_Φ, ρ_{22}, ρ_{33}. So here ESD cannot be avoided by adjusting the strength of reservoir interactions, e.g., the decay rate of q_a and q_b with respect to time.

Fig. 2 (a) is an ESD susceptibility phase diagram of the Φ type of X-form initial state (2) with respect to Q_Φ (C_0) and double excitation D with the single excitations ρ_{22}, ρ_{33} treated as fixed parameters. The black solid line is the ESD-free critical value D_Φ^f, and straightforward calculations show that it can only have cross points with the minimum physical boundary $D_\Phi^{\min}$ when $Q_\Phi = \sqrt{2x_{23}^2 + \Lambda} - 2x_{23}$, and $2D = \sqrt{y_{23}^2 - 2x_{23}^2 + \Lambda} - y_{23}$, with $2\Lambda = 1 - 2y_{23} \pm \sqrt{(1-2y_{23})^2 - 8x_{23}^2}$. Here $-$ and $+$ correspond to points 2 and 3 respectively as illustrated in the plot. From the condition (12), one identifies the region below D_Φ^f in Fig. 2 (a) is the ESD-free phase and everywhere above is the ESD-susceptible phase. Obviously, the double excitation needs to satisfy the relation $D_\Phi^{\min} \leq D \leq D_\Phi^f$ to guarantee an ESD free zone.

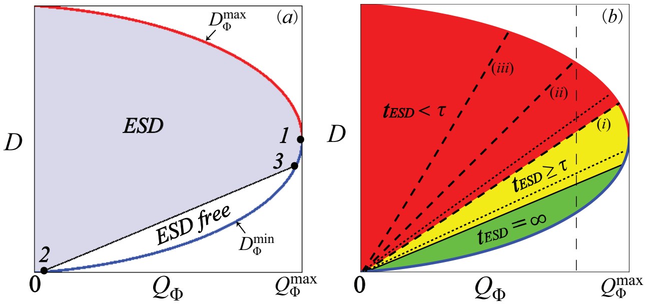

FIG. 2: ESD phase diagrams with respect to the double excitation D and X-matrix entanglement Q_Φ (C_0) for Φ type of initial states. Plot (a) illustrates the ESD-susceptible (shaded) and ESD-free (unshaded) phases separated by the black solid critical line D_Φ^f for X-form initial state (2). Plot (b) is plotted on top of (a), and it illustrates the ESD time phases in the perspective of traffic-light signals. Dashed lines (i), (ii), (iii) represent the ESD-tolerable critical value D_Φ^t for $r = \gamma_a/\gamma_b = 1, 3, 10$ respectively. The green zone below D_Φ^f is the ESD-free (safety) phase. For $r = 1$, the ESD-tolerable (caution) phase is the yellow zone between D_Φ^f and dashed line (i), and the ESD-no-go (danger) phase is the red zone above line (i). The vertical line illustrates $C_0 = Q_\Phi = 0.8$. For the generic state (1), the corresponding ESD-free and ESD-tolerable critical lines will move up a little as schematically shown by lower and upper dotted lines respectively.

We further analyze the ESD onset relation $Q_\Phi(t) = 0$. One can consider a practical situation that quantum computation tasks can tolerate ESD if it happens only after a certain time point τ, which is much longer than the computation and operation time scales, and any ESD that happens earlier than that may be harmful and is considered as a no-go region. Then the ESD-tolerable condition is given as $t_{ESD} \geq \tau$ or $p_k(t_{ESD}) \geq p_k(\tau)$, where $k = a, b$ and t_{ESD} denotes ESD onset time. This relation can be expressed in terms of the double excitation D bounded by its critical value D_Φ^t, i.e.,

$$\begin{aligned} D \leq D_\Phi^t = &\sqrt{\left(\frac{\rho_{22}}{p_b(\tau)} - \frac{\rho_{33}}{p_a(\tau)}\right)^2 + \frac{(Q_\Phi + 2x_{23})^2}{p_a(\tau)p_b(\tau)}} \\ &- \frac{\rho_{22}}{p_b(\tau)} - \frac{\rho_{33}}{p_a(\tau)}. \end{aligned} \quad (13)$$

One can show $\partial D_\Phi^t/\partial p_k(\tau) \leq 0$, i.e., D_Φ^t is a decreasing function of the excitation-transfer probabilities $p_k(\tau)$.

For demonstration, one can reasonably assume the channel dissipation as an exponential decay process, i.e., $p_k(t) = 1 - e^{-\gamma_k t}$, where γ_k ($k = a, b$) are the decay constants for qubits A, B respectively. Then it follows straightforwardly that D_Φ^t is also a decreasing function of γ_k. Fig. 2 (b) illustrates the behavior of D_Φ^t when one fixes channel γ_a and varies the other channel γ_b. The dashed lines (i), (ii), (iii) represent the cases when the ratio $r = \gamma_a/\gamma_b = 1, 3, 10$ respectively. Here τ is taken to be the decay lifetime $1/\gamma_a$. Note that $\gamma_a, \gamma_b = 0$ are singularities of D^t_Φ and they represent the relatively less practical single-channel dissipations. Their ESD-free and ESD-tolerable critical conditions can be obtained easily from (8) and will not be addressed here.

The ESD-susceptible phase in Fig. 2 (a) is then further separated into two phases. In Fig. 2 (b) the green zone is exactly the ESD-free phase in plot (a), and is considered as the safety phase where entanglement decays to zero only at $t_{ESD} = \infty$. For $r = 1$, the ESD-tolerable (caution) phase is the yellow zone where ESD occurs only after the tolerable time scale, i.e., $t_{ESD} \geq \tau$, and the red zone indicates a fast ESD that happens before τ, which is the ESD-no-go (danger) phase that state preparations should avoid. Obviously, this ESD-tolerable region will increase with the increase of the ratio r.

Ψ type of X-matrix

For the Ψ matrix situation, i.e., $C_0 = Q_\Psi > Q_\Phi$. The restriction of Q_Ψ can be achieved as $0 \leq D \leq D^{\max}_\Psi$, where the maximum physical boundary

$$D^{\max}_\Psi = \left(\sqrt{\rho_{22}(4y_{24} - 4y_{24}^2 - Q_\Psi^2)} - Q_\Psi\sqrt{\rho_{44}}\right)^2 /4y_{24}^2 \tag{14}$$

is illustrated in Fig. (3) by the red solid line as a function of Q_Ψ. Under this boundary (14), Q_Ψ takes its maximum value $Q^{\max}_\Psi = 2\sqrt{\rho_{22}(1 - y_{24})}$ when $D = 0$.

From (9) the condition to have ESD is whenever $\Delta(t) + x_{14}^2 \geq |\rho_{23}|^2$. Then the ESD-free condition is achieved as $\Delta_{\max}(t) + x_{14}^2 \leq |\rho_{23}|^2$, which again doesn't depend on the strength of reservoir interactions and can be re-expressed in terms of the double excitation probability bounded by its critical value D^f_Ψ, i.e.,

$$D \leq D^f_\Psi = Q_\Psi^2/4(1 - \sqrt{\rho_{44}})^2. \tag{15}$$

Fig. 3 (a) is an ESD susceptibility phase diagram of the Ψ type of X-form initial state (2) with respect to Q_Ψ (C_0) and double excitation D with the zero excitation ρ_{44} treated as a fixed parameter. The black solid line is the ESD-free critical value D^f_Ψ that separates the ESD-free phase from the ESD-susceptible phase, and it crosses the maximum boundary line $D^{\max}_\Psi$ at a single point (illustrated by point 1 in the plot) when $Q_\Psi = 2(1 - \sqrt{\rho_{44}})\sqrt{\rho_{22}(y_{24} - y_{24}^2)}/\sqrt{\Xi}$ and $D = \rho_{22}(y_{24} - y_{24}^2)/\Xi$, with $\Xi = (\rho_{22} + \sqrt{\rho_{44}})^2 + \rho_{22}(1 - \sqrt{\rho_{44}})^2$. Interestingly, Eq. (15) and Fig. 3 (a) show that when the double excitation vanishes, i.e., $D = 0$, the Ψ type of initial state is ESD free for any amount of Q_Ψ (C_0).

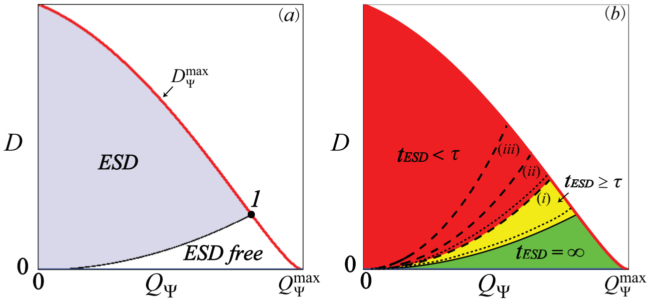

FIG. 3: ESD phase diagrams with respect to the initial double excitation D and X-matrix entanglement Q_Ψ (C_0) for Ψ type of initial states. Plot (a) illustrates the ESD-susceptible (shaded) and ESD-free (unshaded) phases separated by the black solid critical line D^f_Ψ for X-form initial state (2). Plot (b) is a re-plot of (a), and it illustrates the ESD onset time phases in the perspective of traffic-light signals. Dashed lines (i), (ii), (iii) represent the ESD-tolerable critical value D^t_Ψ for $r = \gamma_a/\gamma_b = 1, 3, 10$ respectively. The green zone below the black solid line D^f_Ψ is the ESD-free (safety) phase. For $r = 1$, the ESD-tolerable (caution) phase is the yellow zone between D^f_Ψ and dashed line (i), and the ESD-no-go (danger) phase is the red zone above (i). For the generic state (1), the corresponding ESD-free and ESD-tolerable critical lines will move up a little as schematically shown by lower and upper dotted lines respectively.

From the ESD onset condition $Q_\Psi(t) = 0$, one can again re-express the ESD-tolerable condition $t_{ESD} \geq \tau$ in terms of the double excitation probability as $D \leq D^t_\Psi$. Here D^t_Ψ is the critical value that can be obtained analytically by solving for D from the equation

$$\begin{aligned} Q_\Psi^2/4 &= p_b(\tau)[p_a(\tau) - 1]D^2 - Q_\Psi\sqrt{\rho_{44}D} \\ &+ [\rho_{22}p_a(\tau) + p_b(\tau) - y_{24}p_b(\tau)]D. \end{aligned} \tag{16}$$

The analytic dependence of D^t_Ψ on the parameters Q_Ψ, ρ_{22}, ρ_{44}, $p_a(\tau)$, and $p_b(\tau)$ is a very complicated expression. With the assumptions, $p_k(t) = 1 - e^{-\gamma_k t}$ and $\tau = 1/\gamma_a$, the explicit behavior of D^t_Ψ is illustrated in Fig. 3 (b) by the dashed lines (i), (ii), and (iii) for $r = \gamma_a/\gamma_b = 1, 3, 10$ respectively. In the plot the green zone is exactly the ESD-free zone in plot (a), and it is the safety phase with ESD happens at time infinity. For $r = 1$, the ESD-tolerable (caution) phase is the yellow zone with ESD happens after the tolerable time τ, and the ESD-no-go (danger) phase is the red zone with ESD happens before τ. Again, the ESD-tolerable region increases with the increase of the ratio r.

ESD PHASES FOR ARBITRARY MATRICES

Now we return to the generic initial state (1), and note that the evolutions of $\rho_X(0)$ and $O(0)$ are independent of each other. That is, $\rho_X(t) = \sum_{i=1}^4 K_i(t)\rho_X(0)K_i^\dagger(t)$ remains in an X form as shown in (7), and $O(t) =$

$\sum_{i=1}^{4} K_i(t)O(0)K_i^{\dagger}(t)$ retains the O form, i.e.,

$$O(t) = \begin{pmatrix} 0 & \rho_{12}(t) & \rho_{13}(t) & 0 \\ \rho_{21}(t) & 0 & 0 & \rho_{24}(t) \\ \rho_{31}(t) & 0 & 0 & \rho_{34}(t) \\ 0 & \rho_{42}(t) & \rho_{43}(t) & 0 \end{pmatrix}, \qquad (17)$$

where $\rho_{12}(t) = \rho_{21}^*(t) = \rho_{12} q_a \sqrt{q_b}$, $\rho_{13}(t) = \rho_{31}^*(t) = \rho_{13} q_b \sqrt{q_a}$, $\rho_{24}(t) = \rho_{42}^*(t) = \rho_{24}\sqrt{q_a} + \rho_{13} p_b \sqrt{q_a}$, and $\rho_{34}(t) = \rho_{43}^*(t) = \rho_{34}\sqrt{q_b} + \rho_{12} p_a \sqrt{q_b}$.

Then the analysis in Refs. [16, 17] for static matrices can be extended to the time dependent state $\rho(t) = \rho_X(t) + O(t)$. One immediately notes that the time dependent concurrence of $\rho(t)$ is always no less than that of its X-form component, i.e., $C[\rho(t)] \geq C[\rho_X(t)]$ at any time t. Consequently, the arbitrary state $\rho(0)$ will always reach ESD no earlier than $\rho_X(0)$. This is to say that the exact ESD-free critical conditions (12) and (15) for $\rho_X(0)$ will simply provide lower bounds for those of the entire state $\rho(0)$. Schematic illustrations of those ESD-free critical lines for $\rho(0)$ are provided in Fig. 2 (b) and Fig. 3 (b) by the lower dotted lines, which are guaranteed to be no lower than the corresponding exact ESD-free critical lines D_Φ^f and D_Ψ^f for $\rho_X(0)$. The same argument is also valid for the ESD-tolerable critical conditions, which are schematically illustrated by the upper dotted lines in the corresponding plots for $r = \gamma_a/\gamma_b = 1$. Then the ESD-free, ESD-tolerable and ESD-no-go phases separated by the two dotted critical lines can be identified schematically for the generic initial state (1).

The key information here is that those exact critical conditions for the X-form matrix (2) are sufficient conditions to guarantee the arbitrary state (1) to be ESD free and ESD tolerable respectively. In this sense, the pre-management of ESD properties for the complicated general state $\rho(0)$ can be simply realized by managing just a few parameters that explicitly determine the ESD properties of its X-form component $\rho_X(0)$.

Experimental preparations of initial parameters may not always be precise, e.g., to produce a desired amount of initial entanglement C_0 is a challenge. However, our ESD phase analysis shows that one is still able to control the ESD properties within a range of these parameters. To be more specific, let us take the Φ type of X-form component $\rho_X(0)$ as an example. Suppose the experimenter is able to prepare initial entanglement within the range $0.80 \leq C_0 \leq 0.96$. This requires very small single excitations, e.g., $\rho_{22} = \rho_{33} = 0.01$. Some simple arithmetic shows that $D_\Phi^{\max} \simeq 0.76$, $D_\Phi^t \simeq 0.63$ (r=1), $D_\Phi^f \simeq 0.40$, and $D_\Phi^{\min} \simeq 0.22$ for the lower bound case $C_0 = 0.8$, illustrated by the vertical dashed line in Fig. 2 (b). Then the ESD-free, ESD-tolerable phases can be realized when the experimenter controls the double excitation in the ranges $0.22 \leq D \leq 0.40$, $0.40 \leq D \leq 0.63$ respectively.

The monotonic increasing nature (with respect to C_0) of critical values D_Φ^f and D_Φ^t indicates that the preferred ranges of D for $C_0 = 0.8$ will guarantee the corresponding ESD properties for states with $C_0 \geq 0.8$. Moreover, those ranges are also guaranteed to assure the corresponding ESD properties for the generic state $\rho(0)$.

CONCLUSION

In summary we have studied possible pre-management of non-local decoherence, i.e., ESD susceptibility and timing, with limited resources of initial conditions. This is an open question not only from the view of fundamental entanglement theory, but also from the practical aspect of preparing robust entangled states.

It is easy to imagine that ESD properties may relate, at least partially, to initial conditions. However, to pre-manage them for arbitrarily complicated states with just a few initial parameters is not so intuitive. Our results show that it is possible to realize such a pre-management through initial entanglement and excitation probabilities for a generic two-qubit state that undergoes local different amplitude damping dissipations. These parameters just amount to a set of management tools that control the critical conditions for ESD-free, ESD-tolerable, and ESD-no-go phases of the state. In addition, these phases allow a well defined amount of margin for errors in practical imprecise state preparations.

We remark that the cases when the environmental noises are of phase-damping or mixed-damping mechanisms will show similar ESD phases. These will simply enlarge the picture of pre-manageable ESD phenomenon and will be addressed elsewhere.

ACKNOWLEDGEMENT

The author would like to acknowledge discussions with J.H. Eberly as well as partial financial support from the following agencies: DARPA HR0011-09-1-0008, ARO W911NF-09-1-0385, NSF PHY-0855701.

---

[*] Electronic address: xfqian@pas.rochester.edu

[1] M. A. Nielsen and I. L. Chuang, *Quantum Computation and Quantum Information* (Cambridge Univ. Press, 2000); and J. Preskill, *Quantum Information and Computation*, Caltech Lecture Notes for Ph219/CS219.

[2] W.H. Zurek, Phys. Today **44**, 38 (1991); W. H. Zurek, Rev. Mod. Phys. **75**, 715 (2003).

[3] K. Zyczkowski, P. Horodecki, M. Horodecki, and R. Horodecki, Phys. Rev. A **65**, 012101 (2001); A.K. Rajagopal and R.W. Rendell, Phys. Rev. A **63**, 022116 (2001); T. Yu and J.H. Eberly, Phys. Rev. B **68**, 165322 (2003); L. Diósi, in *Irreversible Quantum Dynamics*, edited by F. Benatti and R. Floreanini (Lecture notes in physics, Vol 622), (Springer-Verlag, Berlin, 2003), p.

157; P.J. Dodd and J.J. Halliwell, Phys. Rev. A **69**, 052105 (2004).

[4] T. Yu and J.H. Eberly, Phys. Rev. Lett. **93**, 140404 (2004); T. Yu and J.H. Eberly, Science **323**, 598 (2009).

[5] P.W. Shor, Phys. Rev. A **52**, R2493 (1995).

[6] H.M. Wiseman and G.J. Milburn, Phys. Rev. Lett. **70**, 548 (1993).

[7] L. Viola and S. Lloyd, Phys. Rev. A **58**, 2733 (1998).

[8] T. Yu and J.H. Eberly, Phys. Rev. Lett. **97**, 140403 (2006).

[9] I. Sainz and G. Björk , Phys. Rev. A **77**, 052307 (2008); M. Yönaç and J.H. Eberly, arXiv: 1211.5654 (2012).

[10] Y. Li, B. Luo, and H. Guo, Phys. Rev. A **84**, 012316 (2011).

[11] S.K. Goyal, S. Banerjee, and S. Ghosh, Phys. Rev. A **85**, 012327 (2012).

[12] G.M. Palma, K.A. Suominen, and A.K. Ekert, Proc. R. Soc. London, Ser. A **452**, 567 (1996); P. Zanardi and M. Rasetti, Phys. Rev. Lett. **79**, 3306 (1997); D.A. Lidar, I.L. Chuang, and K.B. Whaley, Phys. Rev. Lett. **81**, 2594 (1998).

[13] P. Zanardi, Phys. Lett. A **258**, 77 (1999); L. Viola, E. Knill, and S. Lloyd, Phys. Rev. Lett. **82**, 2417 (1999).

[14] X.-F. Qian and J.H. Eberly, Phys. Lett. A **376**, 2931 (2012).

[15] K.M. Fonseca-Romero, J. Martínez-Rincón, and C. Viviescas, Phys. Rev. A **86**, 042325 (2012).

[16] Z.-H. Ma, Z.-H. Chen, J.-L. Chen, C. Spengler, A. Gabriel, and M. Huber, Phys. Rev. A **83**, 062325 (2011).

[17] S.M. Hashemi Rafsanjani and S. Agarwal, arXiv: 1204.3912 (2012).

[18] T. Yu and J.H. Eberly, Quant. Inf. Comp. **7**, 459 (2007).

[19] W.K. Wootters, Phys. Rev. Lett. **80**, 2245 (1998).

[20] For example, see S. Bose, Phys. Rev. Lett. **91**, 207901 (2003); X.-F. Qian, Y. Li, Y. Li, Z. Song, and C.P. Sun, Phys. Rev. A **72**, 062329 (2005).